PERGAMON

Computers & Fluids 29 (2000) 951–979

computers & fluids

www.elsevier.com/locate/compfluid

On numerical treatment of the source terms in the shallow water equations

P. Garcia-Navarro[a], M.E. Vazquez-Cendon[b,*]

[a]*Fluid Mechanics C.P.S., University of Zaragoza, Zaragoza 50015, Spain*
[b]*Department of Applied Mathematics, University of Santiago de Compostela, Santiago de Compostela, Spain*

Received 4 May 1998; received in revised form 5 July 1999; accepted 22 July 1999

Abstract

Upwind schemes are very well adapted to advection dominated flows and have become popular for applications involving the Euler system of equations. Recently, Riemann solver-based techniques such as Roe's scheme have become a successful tool for numerical simulation of other conservation laws like the shallow water equations. One of the disadvantages of this technique is related to the treatment of the source terms of the equations. The conservativity of the scheme can be seriously damaged if a careless treatment is applied. Previous papers studied the way to treat the terms arising from bed level changes. This paper deals with the analysis of the main reasons leading to a correct treatment of the geometrical source terms, that is, those representing the changes in cross-section which may be linked to the specific dependence of the flux function on the geometry.

Keywords: Source terms; Shallow water equations; Roe's scheme; Channel with irregular geomatries; Shallow water equations

1. Introduction

The explicit first-order Roe's scheme is very popular in Gas Dynamics and has been frequently reported in shallow water applications mainly in relation to advection dominated flows [10]. The discretization of the source terms is usually done following pointwise or upwind approaches. Vazquez-Cendon [11] showed that the upwinding approach was an improvement

* Corresponding author. Tel.: +34-981-563100; fax: +34-981-597054.
E-mail address: elena@zmat.usc.es (M.E. Vazquez-Cendon).

0045-7930/00/$ - see front matter
PII: S0045-7930(99)00038-9

over the pointwise method for problems involving constant rectangular cross-section and bed level variation. The cross-sectional shape variation was not considered in that work. In this paper, it will be shown to perform rather poorly when an extension of the technique is considered as applied to the shallow water equations with dominant source terms arising from width variation. The scheme fails to reproduce the steady state of still water in a rectangular channel with variations in bed slope and width. For a simple physical problem where the solution is just a horizontal water level at rest, the scheme results in considerable oscillations in the water levels and non-negligible discharges caused by poor treatment of the source terms. In this paper, we adapt the upwind approach to overcome these difficulties. The work is related to some recent contributions such as [8] and [9].

The starting point will be a homogeneous system representing a conservation law

$$\frac{\partial \mathbf{U}}{\partial t} + \frac{\partial \mathbf{F}(\mathbf{x}, \mathbf{U})}{\partial x} = 0$$

where the conserved variables are $\mathbf{U}$, their fluxes are $\mathbf{F}(\mathbf{x}, \mathbf{U})$ and the Jacobian matrix will be denoted by $\mathbf{J}$, where

$$\mathbf{J} = \frac{\partial \mathbf{F}(\mathbf{x}, \mathbf{U})}{\partial \mathbf{U}}.$$

The construction of Roe's scheme is based on a local linearization that requires the definition of an analytic Jacobian [10]. For this discrete representation of the system, it is necessary that the condition

$$\Delta \mathbf{F} = \mathbf{J} \Delta \mathbf{U} \tag{1}$$

holds among spatial increments of the variables $\mathbf{F}$ and $\mathbf{U}$.

The case of a prismatic channel of rectangular cross-section will be presented first as it is the simplest case and the only one in which condition (1) holds. Then, the rectangular non-prismatic case will illustrate where the problem is, and a way to solve it. Numerical results for a laboratory experiment involving unsteady flow over abrupt changes in slope will also be presented. As a supplementary example, the scheme will be applied to a scalar case related to solute transport in shallow water.

Roe's first-order explicit scheme can have a dual interpretation, either, based on a fluctuation-signal model or on a numerical flux model. Both the approaches have always been considered equivalent for 1D cases. This is true in the case $\mathbf{F} = \mathbf{F}(\mathbf{U})$ and no spatial dependence in $\mathbf{F}$. The second version is usually found in the Riemann solvers and conservative schemes literature and often applied in the context of 2D extensions via finite volumes. The first one is, however, preferable to extend the scheme to $CFL > 1$ and to progress to multi-dimensional upwinding in 2D. In the second section of this paper, it will be pointed out that the two approaches differ also in 1D cases in which there are cross-section variation in space, that is, cases that may introduce a spatial dependence in the flux function $\mathbf{F}$. In case of a trapezoidal cross-section, for instance, this dependence cannot be avoided.

2. Numerical discretization of a 1D system

2.1. First-order Roe's method

Provided that Roe's linearization [10] is used to decouple the homogeneous part of a system like

$$\frac{\partial \mathbf{U}}{\partial t} + \frac{\partial \mathbf{F}(\mathbf{x}, \mathbf{U})}{\partial x} = \mathbf{R}(\mathbf{x}, \mathbf{U}), \tag{2}$$

an approximate matrix $\tilde{\mathbf{J}}$ can be built whose eigenvalues $\tilde{\lambda}_k$ and eigenvectors $\tilde{\mathbf{e}}_k$ satisfy for every pair of nodal points $(i, i+1)$ in a 1D computational grid

$$\Delta \mathbf{U}_{i+\frac{1}{2}} = \mathbf{U}_{i+1} - \mathbf{U}_i = \sum_k (\tilde{\alpha}_k \tilde{\mathbf{e}}_k)_{i+\frac{1}{2}} \tag{3}$$

$$\Delta \mathbf{F}_{i+\frac{1}{2}} = \mathbf{F}_{i+1} - \mathbf{F}_i = \tilde{\mathbf{J}}_{i+\frac{1}{2}} \Delta \mathbf{U}_{i+\frac{1}{2}} \tag{4}$$

$$\tilde{\mathbf{J}}_{i+\frac{1}{2}} \Delta \mathbf{U}_{i+\frac{1}{2}} = \sum_k \left(\tilde{\lambda}_k \tilde{\alpha}_k \tilde{\mathbf{e}}_k\right)_{i+\frac{1}{2}}. \tag{5}$$

They have a formal expression similar to the eigenvectors and eigenvalues of the analytical Jacobian in terms of average quantities. However, the average quantities are defined, the basic idea is to calculate $\Delta \mathbf{U}$ at every interface and propagate the different k waves according to the sign of their eigenvalues and the values of the local CFL numbers ν_k. As an example, if at $i+\frac{1}{2}$, for $k=1$, $(\tilde{\lambda}_1)_{i+\frac{1}{2}} > 0$, then each component of the fluctuation $\Delta \mathbf{U}$, ΔU_j, $j=1,2$, will affect the corresponding variable U_j so that, the signal

$\left(\nu_1 \tilde{\alpha}_1 \tilde{e}_{1j}\right)_{i+\frac{1}{2}}$ is added to $i+1$

where

$$\nu_1 = \frac{\Delta t}{\Delta x} \left(\tilde{\lambda}_1\right)_{i+\frac{1}{2}}$$

At the end, for the homogeneous problem ($\mathbf{R}(\mathbf{x}, \mathbf{U}) = 0$), every computational node gets a total contribution

$$\mathbf{U}_i^{n+1} = \mathbf{U}_i^n - \frac{\Delta t}{\Delta x}\left(\left(\tilde{\lambda}_1^- \tilde{\alpha}_1 \tilde{\mathbf{e}}_1\right)_{i+\frac{1}{2}} + \left(\tilde{\lambda}_2^- \tilde{\alpha}_2 \tilde{\mathbf{e}}_2\right)_{i+\frac{1}{2}} + \left(\tilde{\lambda}_1^+ \tilde{\alpha}_1 \tilde{\mathbf{e}}_1\right)_{i-\frac{1}{2}} + \left(\tilde{\lambda}_2^+ \tilde{\alpha}_2 \tilde{\mathbf{e}}_2\right)_{i-\frac{1}{2}}\right) \tag{6}$$

where

$$\tilde{\lambda}_k^{\pm} = \frac{1}{2}\left(\tilde{\lambda}_k \pm |\tilde{\lambda}_k|\right) \tag{7}$$

This version of Roe's first order scheme will be addressed as the signal model. There is an alternative presentation of the scheme that is even more widespread, it is the numerical flux model. It is based on the definition of a numerical flux characteristic of the conservative schemes. Using the definition of $\tilde{\lambda}_k^{\pm}$ (7)

$$\mathbf{U}_i^{n+1} = \mathbf{U}_i^n - \frac{\Delta t}{2\Delta x}\left[\sum_k \left(\tilde{\lambda}_k \tilde{\alpha}_k \tilde{\mathbf{e}}_k\right)_{i+\frac{1}{2}} + \sum_k \left(\tilde{\lambda}_k \tilde{\alpha}_k \tilde{\mathbf{e}}_k\right)_{i-\frac{1}{2}} - \sum_k \left(|\tilde{\lambda}_k| \tilde{\alpha}_k \tilde{\mathbf{e}}_k\right)_{i+\frac{1}{2}} + \sum_k \left(|\tilde{\lambda}_k| \tilde{\alpha}_k \tilde{\mathbf{e}}_k\right)_{i-\frac{1}{2}}\right] \tag{8}$$

This expression is then transformed into

$$\mathbf{U}_i^{n+1} = \mathbf{U}_i^n - \frac{\Delta t}{\Delta x}\left(\mathbf{f}^*_{i+\frac{1}{2}} - \mathbf{f}^*_{i-\frac{1}{2}}\right)$$

with a numerical flux function crossing every interface

$$\mathbf{f}^*_{i+\frac{1}{2}} = \frac{1}{2}(\mathbf{F}_i + \boldsymbol{F}_{i+1}) - \frac{1}{2}\sum_k \left(|\tilde{\lambda}_k| \tilde{\alpha}_k \tilde{\mathbf{e}}_k\right)_{i+\frac{1}{2}} \tag{9}$$

using Eq. (1), that is, using as the necessary condition,

$$\sum_k \left(\tilde{\lambda}_k \tilde{\alpha}_k \tilde{\mathbf{e}}_k\right)_{i+\frac{1}{2}} = \Delta \mathbf{F}_{i+\frac{1}{2}} = \mathbf{F}_{i+1} - \mathbf{F}_i$$

2.2. Discretization of the source terms

There are two ways of dealing with the source terms found in the partial differential equations. These are, the pointwise approach, i.e. evaluation of the source term functions at the grid point, and the upwind approach, that is, projection of the source terms onto the basis of eigenvectors. We will comment on both of them and compare their performance.

2.2.1. Pointwise approach

The simplest pointwise option for a generic source term function $\mathbf{R}(x, \mathbf{U})$ can be expressed as:

$$\mathbf{R}_i \approx \mathbf{R}\left(\mathbf{x}_i, \mathbf{U}_i^n\right)$$

which consists of a simple evaluation at the nodal point using the already known dependent variables. Other possibilities also include some form of average between neighbouring nodal points. Firstly, all signals are propagated to update the dependent variables as described in the previous section, then the source terms are added to the updated variables.

Problems may arise, however, when the source term contains spatial derivatives and a definition of their discrete representation must be established. This difficulty will be met for the discretization of the bottom slope (S_0) and variable width (I_2) source terms.

2.2.2. Upwind approach

The upwind approach for the treatment of the source terms is based on the reasoning that the homogeneous system can be discretized as in (6) so that

$$\mathbf{U}_i^{n+1} - \mathbf{U}_i^n + \frac{\Delta t}{\Delta x}\left[\left(\sum_{k+}\tilde{\lambda}_k\tilde{\alpha}_k\tilde{\mathbf{e}}_k\right)_{i-\frac{1}{2}} + \left(\sum_{k-}\tilde{\lambda}_k\tilde{\alpha}_k\tilde{\mathbf{e}}_k\right)_{i+\frac{1}{2}}\right] = 0$$

where $k\pm$ indicate the positive or negative eigenvalues, i.e. wave speeds, at every interface.

Then, the source terms can be discretized as

$$\mathbf{R}\Delta x = \sum_k \tilde{\beta}_k\tilde{\mathbf{e}}_k. \tag{10}$$

The signal that is propagated to alter the variables at the nodes is modified by the influence of the source terms always according to the signs of the local wave speed (eigenvalue), and the discretization of the system becomes:

$$\mathbf{U}_i^{n+1} = \mathbf{U}_i^n - \frac{\Delta t}{\Delta x}\left[\left(\sum_{k+}\left(\tilde{\lambda}_k\tilde{\alpha}_k - \tilde{\beta}_k\right)\tilde{\mathbf{e}}_k\right)_{i-\frac{1}{2}} + \left(\sum_{k-}\left(\tilde{\lambda}_k\tilde{\alpha}_k - \tilde{\beta}_k\right)\tilde{\mathbf{e}}_k\right)_{i+\frac{1}{2}}\right] \tag{11}$$

The upwind philosophy of this decomposition of the source terms becomes clearer following the notation introduced by Bermudez and Vazquez-Cendon [3]. The source term influencing node i consists of a part from the left half cell and another from the right half cell. The upwind discretization determines the relative amount of these two parts. Expression (10) can be rewritten as

$$\mathbf{R}\Delta x = \mathbf{X}\boldsymbol{\beta}$$

where

$$\mathbf{X} = \begin{pmatrix} 1 & 1 \\ \lambda_1 & \lambda_2 \end{pmatrix} \qquad \boldsymbol{\beta} = \begin{pmatrix} \beta_1 \\ \beta_2 \end{pmatrix}.$$

Matrix $\mathbf{X}$ has the property of diagonalising the Jacobian of the system

$$\boldsymbol{\Lambda} = \mathbf{X}^{-1}\mathbf{J}\mathbf{X} = \begin{pmatrix} \lambda_1 & 0 \\ 0 & \lambda_2 \end{pmatrix}$$

However, it is possible to write

$$\mathbf{R}\Delta x = \mathbf{X}\boldsymbol{\beta} = \mathbf{X}\boldsymbol{\Lambda}\boldsymbol{\Lambda}^{-1}\boldsymbol{\beta} = \mathbf{X}\boldsymbol{\Lambda}^{+}\boldsymbol{\Lambda}^{-1}\boldsymbol{\beta} + \mathbf{X}\boldsymbol{\Lambda}^{-}\boldsymbol{\Lambda}^{-1}\boldsymbol{\beta}$$

with

$$\boldsymbol{\Lambda}^{\pm} = \frac{1}{2}(\boldsymbol{\Lambda} \pm |\boldsymbol{\Lambda}|) \quad \text{and} \quad |\boldsymbol{\Lambda}| = \begin{pmatrix} |\lambda_1| & 0 \\ 0 & |\lambda_2| \end{pmatrix}.$$

The contribution to nodal point i is written as a sum of left and right portions ψ_L and ψ_R. On a uniform mesh

$$\mathbf{R}_i\Delta_x = \frac{1}{\Delta x}\left(\frac{\Delta x}{2}(\boldsymbol{\psi}_L)_{i-\frac{1}{2}} + \frac{\Delta x}{2}(\boldsymbol{\psi}_R)_{i+\frac{1}{2}}\right) = \frac{1}{2}\left((\mathbf{H}_L\boldsymbol{\beta})_{i-\frac{1}{2}} + (\mathbf{H}_R\boldsymbol{\beta})_{i+\frac{1}{2}}\right) \tag{12}$$

where

$$\mathbf{H}_L = \begin{pmatrix} 1+s_1 & 1+s_2 \\ \tilde{\lambda}_1(1+s_1) & \tilde{\lambda}_2(1+s_2) \end{pmatrix} \qquad \mathbf{H}_R = \begin{pmatrix} 1-s_1 & 1-s_2 \\ \tilde{\lambda}_1(1-s_1) & \tilde{\lambda}_2(1-s_2) \end{pmatrix}.$$

In the above expressions

$$\boldsymbol{\psi}_L = \tilde{\beta}\begin{pmatrix} s_1 - s_2 \\ \tilde{\lambda}_1(1+s_1) - \tilde{\lambda}_2(1+s_2) \end{pmatrix} \qquad \boldsymbol{\psi}_R = \tilde{\beta}\begin{pmatrix} s_2 - s_1 \\ \tilde{\lambda}_1(1-s_1) - \tilde{\lambda}_2(1-s_2) \end{pmatrix}$$

and $s_k = \text{sign}(\tilde{\lambda}_k)$. These are all equivalent formulations.

In the context of the numerical flux formulation, the upwind source terms are incorporated as follows:

$$\mathbf{U}_i^{n+1} = \mathbf{U}_i^n - \frac{\Delta t}{\Delta x}\left(\mathbf{f}^*_{i+\frac{1}{2}} - \boldsymbol{f}^*_{i-\frac{1}{2}}\right) + \Delta t\left(\frac{1}{2}(\boldsymbol{\psi}_L)_{i-\frac{1}{2}} + \frac{1}{2}(\boldsymbol{\psi}_R)_{i+\frac{1}{2}}\right) \tag{13}$$

2.3. Roe's scheme when $\mathbf{F} = \mathbf{F}(\mathbf{x}, \mathbf{U})$

In this case, when the flux of the conserved variables contains an extra dependence, what happens is

$$\Delta\mathbf{F} \neq \mathbf{J}\Delta\mathbf{U}$$

instead

$$\Delta\mathbf{F} = \mathbf{J}\Delta\mathbf{U} + \mathbf{V} \tag{14}$$

The flux discretization (6) only considers the part $\mathbf{J}\Delta\mathbf{U}$, then it is necessary to move the term $\mathbf{V}$ to the right hand side of the equations. Given the form of this extra source term, the flux is corrected because $\boldsymbol{V}$ is subtracted from $\boldsymbol{\Delta}\mathbf{F}$ and added to the source terms

$$\hat{\mathbf{R}} = \mathbf{R} - \mathbf{V} \tag{15}$$

The final form of the source term is then upwinded according to the previous scheme. On the other hand, whenever the flux function depends also on $\mathbf{x}$, it is necessary to introduce the corresponding corrections in the numerical flux. In this case,

$$\sum_k \left(\tilde{\lambda}_k\tilde{\alpha}_k\tilde{\mathbf{e}}_k\right)_{i+\frac{1}{2}} = \Delta\mathbf{F}_{i+\frac{1}{2}} - \mathbf{V}_{i+\frac{1}{2}} = \mathbf{F}_{i+1} - \mathbf{F}_i - \mathbf{V}_{i+\frac{1}{2}}$$

Thus,

$$\mathbf{U}_i^{n+1} = \mathbf{U}_i^n - \frac{\Delta t}{\Delta x}\left[\frac{1}{2}\left(\mathbf{F}_i + \mathbf{F}_{i+1} + \mathbf{V}_{i+\frac{1}{2}}\right) - \frac{1}{2}\sum_k \left(|\tilde{\lambda}_k|\tilde{\alpha}_k\tilde{\mathbf{e}}_k\right)_{i+\frac{1}{2}} - \frac{1}{2}\left(\mathbf{F}_i + \mathbf{F}_{i-1} - \mathbf{V}_{i-\frac{1}{2}}\right) + \frac{1}{2}\sum_k \left(|\tilde{\lambda}_k|\tilde{\alpha}_k\tilde{\mathbf{e}}_k\right)_{i-\frac{1}{2}}\right]. \tag{16}$$

The definition of a corrected numerical flux becomes

$$\tilde{\mathbf{f}}^*_{i+\frac{1}{2}} = \frac{1}{2}\left(\mathbf{F}_i + \mathbf{F}_{i+1} + \mathbf{V}_{i+\frac{1}{2}}\right) - \frac{1}{2}\sum_k \left(|\tilde{\lambda}_k|\tilde{\alpha}_k\tilde{\mathbf{e}}_k\right)_{i+\frac{1}{2}} \tag{17}$$

$$\tilde{\mathbf{f}}^*_{i-\frac{1}{2}} = \frac{1}{2}\left(\mathbf{F}_i + \mathbf{F}_{i-1} - \mathbf{V}_{i-\frac{1}{2}}\right) - \frac{1}{2}\sum_k \left(|\tilde{\lambda}_k|\tilde{\alpha}_k\tilde{\mathbf{e}}_k\right)_{i-\frac{1}{2}} \tag{18}$$

3. The shallow-water equations

The shallow water or St. Venant equations are a simplified model of some free surface flows whose derivation can be found in [5], or in [1]. They can be written as the following system of equations:

$$\frac{\partial A}{\partial t} + \frac{\partial Q}{\partial x} = 0$$

$$\frac{\partial Q}{\partial t} + \frac{\partial}{\partial x}\left(\frac{Q^2}{A} + gI_1\right) = gI_2 + gA\left(S_0 - S_f\right). \tag{19}$$

This is a conservative formulation where $A = A(x, t)$ is the wetted cross-sectional area (see Fig. 1)

$$A(x, t) = \int_0^{h(x,\,t)} \sigma(x, \eta)\,\mathrm{d}\eta$$

$$\sigma(x, h) = b(x),$$

$Q = Q(x, t)$ is the discharge and g is the acceleration due to gravity. I_1 represents a hydrostatic pressure force term

$$I_1 = \int_0^{h(x,\,t)} (h - \eta)\sigma(x, \eta)\,\mathrm{d}\eta$$

in a section of water level surface h and width

$$\sigma(x,\eta)=\frac{\partial A(x,t)}{\partial \eta}$$

and I_2 accounts for the pressure forces in a volume of constant depth h due to longitudinal width variations,

$$I_2=\int_0^{h(x,t)}(h-\eta)\frac{\partial \sigma(x,\eta)}{\partial x}\,\mathrm{d}\eta.$$

According to the definitions of I_1 and I_2, and following Leibnitz's rule of derivation of an integral,

$$\frac{\partial I_1}{\partial x}=I_2+A\frac{\partial h}{\partial x} \tag{20}$$

The bed slope is the spatial partial derivative of the bottom elevation z,

$$S_0=-\frac{\mathrm{d}z}{\mathrm{d}x}$$

and the last term contains the effects of viscosity through friction with the solid surfaces. The quantity S_f denotes the energy grade line and can be expressed in terms of the rest of the variables of interest by means of semiempirical expressions such as Manning or Chezy's laws [5].

It is possible to rewrite the Eqs. (19) in the form:

$$\frac{\partial \mathbf{U}}{\partial t}+\frac{\partial \mathbf{F}(\mathbf{x},\mathbf{U})}{\partial x}=\mathbf{R}(\mathbf{x},\mathbf{U}) \tag{21}$$

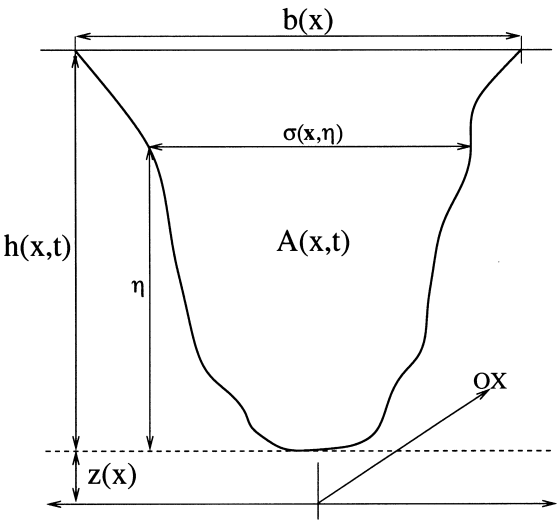

Fig. 1. Cross-sectional geometry.

so that

$$\mathbf{U} = (A, Q)^{\mathrm{T}}$$

$$\mathbf{F} = \left(Q, \frac{Q^2}{A} + gI_1\right)^{\mathrm{T}}$$

$$\mathbf{R} = \left(0, gI_2 + gA\left(S_0 - S_f\right)\right)^{\mathrm{T}},$$

The Jacobian matrix of this system is

$$\mathbf{J} = \frac{\partial \mathbf{F}}{\partial \mathbf{U}} = \begin{pmatrix} 0 & 1 \\ g\dfrac{A}{b} - \dfrac{Q^2}{A^2} & 2\dfrac{Q}{A} \end{pmatrix} = \begin{pmatrix} 0 & 1 \\ c^2 - u^2 & 2u \end{pmatrix},$$

where it has been used that, in general,

$$\frac{\partial I_1}{\partial A} = \frac{A}{b} \quad \text{and} \quad c = \sqrt{g\frac{A}{b}}. \tag{22}$$

The eigenvalues and eigenvectors of $\mathbf{J}$ are:

$$\lambda^{1,2} = u \pm c$$

$$\mathbf{e}^{1,2} = (1, u \pm c)^{\mathrm{T}}.$$

3.1. Flow in a constant width rectangular channel

In the case of rectangular cross-section of constant breadth

$$I_1 = \frac{A^2}{2b}, \qquad I_2 = 0.$$

so that, neglecting friction for the moment

$$\mathbf{U} = (A, Q)^{\mathrm{T}}$$

$$\mathbf{F} = \left(Q, \frac{Q^2}{A} + \frac{gA^2}{2b}\right)^{\mathrm{T}}$$

$$\mathbf{R} = (0, gAS_0)^{\mathrm{T}}.$$

In order to check condition (1)

$$\Delta\mathbf{U} = \begin{pmatrix} \Delta A \\ \Delta Q \end{pmatrix} \Longrightarrow \mathbf{J}\Delta\mathbf{U} = \begin{pmatrix} \Delta Q \\ \left(g\frac{A}{b} - \frac{Q^2}{A^2}\right)\Delta A + 2\frac{Q}{A}\Delta Q \end{pmatrix}$$

On the other hand

$$\Delta\mathbf{F} = \begin{pmatrix} \Delta Q \\ \Delta\left(\frac{Q^2}{A}\right) + \frac{g}{2b}\Delta(A^2) \end{pmatrix} = \begin{pmatrix} \Delta Q \\ \left(g\frac{A}{b} - \frac{Q^2}{A^2}\right)\Delta A + 2\frac{Q}{A}\Delta Q \end{pmatrix}$$

so that in this case it is true that

$$\Delta\mathbf{F} = \mathbf{J}\Delta\mathbf{U}$$

since $\mathbf{F} = \mathbf{F}(\mathbf{U})$. The consequence is that, for the flux discretization, Roe's scheme, as has been described, performs well as in [2].

3.2. Non-prismatic rectangular channel

When the rectangular channel has a variable width

$$\frac{\partial b}{\partial x} = b_x \neq 0$$

the conservative system is formed by

$$\mathbf{U} = (A, Q)^{\mathrm{T}}$$

$$\mathbf{F} = \left(Q, \frac{Q^2}{A} + \frac{gA^2}{2b}\right)^{\mathrm{T}}$$

$$\mathbf{R} = (0, gI_2 + gAS_0)^{\mathrm{T}}, \tag{23}$$

where now

$$I_2 = \frac{A^2}{2b^2}b_x$$

The Jacobian matrix of the system is the same as before and we can repeat:

$$\Delta\mathbf{U} = \begin{pmatrix} \Delta A \\ \Delta Q \end{pmatrix} \Longrightarrow \mathbf{J}\Delta\mathbf{U} = \begin{pmatrix} \Delta Q \\ \left(g\frac{A}{b} - \frac{Q^2}{A^2}\right)\Delta A + 2\frac{Q}{A}\Delta Q \end{pmatrix}$$

But now $\mathbf{F} = \mathbf{F}(\mathbf{x}, \mathbf{U})$ and

$$\Delta\mathbf{F} = \begin{pmatrix} \Delta Q \\ \Delta\left(\frac{Q^2}{A}\right) + \frac{g}{2}\Delta\left(\frac{A^2}{b}\right) \end{pmatrix} = \begin{pmatrix} \Delta Q \\ \left(g\frac{A}{b} - \frac{Q^2}{A^2}\right)\Delta A + 2\frac{Q}{A}\Delta Q - \frac{gA^2}{2b^2}\Delta b \end{pmatrix}$$

that is, now

$$\mathbf{V} = \begin{pmatrix} 0 \\ -\frac{gA^2}{2b^2}\Delta b \end{pmatrix}. \tag{24}$$

4. Application of Roe's scheme to the shallow water equations

4.1. Prismatic channel: $\mathbf{F} = \mathbf{F}(\mathbf{U})$

The approximate Riemann solver is based on some average quantities $\tilde{u}$, $\tilde{c}$, in terms of which the eigenvalues and eigenvectors of the approximate Jacobian are expressed

$$\tilde{\lambda}_{1,\,2} = \tilde{u} \pm \tilde{c}$$

$$\tilde{\mathbf{e}}_{1,\,2} = (1,\, \tilde{u} \pm \tilde{c})^{\mathrm{T}}.$$

Using (3) and omitting the subscripts for the sake of clarity

$$\Delta A = \tilde{\alpha}_1 + \tilde{\alpha}_2$$

$$\Delta Q = \tilde{\alpha}_1(\tilde{u} + \tilde{c}) + \tilde{\alpha}_2(\tilde{u} - \tilde{c})$$

the coefficients are then

$$\tilde{\alpha}_1 = \frac{(\tilde{c} - \tilde{u})\Delta A + \Delta Q}{2\tilde{c}} \qquad \tilde{\alpha}_2 = \frac{(\tilde{c} + \tilde{u})\Delta A - \Delta Q}{2\tilde{c}}$$

In order to determine the average velocity and celerity, $\tilde{u}$ and $\tilde{c}$, from Eq. (5) we write

$$\Delta Q = \tilde{\lambda}_1\tilde{\alpha}_1 + \tilde{\lambda}_2\tilde{\alpha}_2$$

$$\left(g\frac{A}{b} - \frac{Q^2}{A}\right)\Delta A + 2\frac{Q}{A}\Delta Q = \tilde{\lambda}_1\tilde{\alpha}_1(\tilde{u} + \tilde{c}) + \tilde{\lambda}_2\tilde{\alpha}_2(\tilde{u} - \tilde{c}) = 2\tilde{u}\Delta Q + \left(\tilde{c}^2 - \tilde{u}^2\right)\Delta\mathrm{A}$$

The first is just an identity. From the second, values of the averages wanted can be found requiring two separate conditions

$$g\frac{A}{b}\Delta A = \tilde{c}^2\Delta A$$

$$-\frac{Q^2}{A}\Delta A + 2\frac{Q}{A}\Delta Q = 2\tilde{u}\Delta Q - \tilde{u}^2\Delta A$$

so that the following definitions can be stated [7]

$$\tilde{u}_{i+\frac{1}{2}} = \frac{Q_{i+1}\sqrt{A_i} + Q_i\sqrt{A_{i+1}}}{\sqrt{A_i A_{i+1}}\left(\sqrt{A_{i+1}} + \sqrt{A_i}\right)} \tag{25}$$

$$\tilde{c}_{i+\frac{1}{2}} = \sqrt{\frac{g}{2}\left(\left(\frac{A}{b}\right)_i + \left(\frac{A}{b}\right)_{i+1}\right)} \tag{26}$$

The decomposition of the source terms can be expressed as

$$\mathbf{R} = \begin{pmatrix} 0 \\ g\left(-\tilde{A}z_x - \tilde{A}\tilde{S}_f + \frac{\tilde{A}^2}{2\tilde{b}^2}b_x\right) \end{pmatrix} = \frac{1}{\Delta x}\left(\tilde{\beta}_1\begin{pmatrix} 1 \\ \tilde{u}+\tilde{c} \end{pmatrix} + \tilde{\beta}_2\begin{pmatrix} 1 \\ \tilde{u}-\tilde{c} \end{pmatrix}\right)$$

giving

$$\tilde{\beta}_1 = -\tilde{\beta}_2 = \tilde{\beta}$$

where

$$\tilde{\beta} = \frac{\Delta x}{2\tilde{c}}g\left(-\tilde{A}z_x - \tilde{A}\tilde{S}_f + \frac{\tilde{A}^2}{2\tilde{b}^2}b_x\right) = \frac{g}{2\tilde{c}}\left(-\tilde{A}\Delta z - \tilde{A}\Delta x\tilde{S}_f + \frac{\tilde{A}^2}{2\tilde{b}^2}\Delta b\right). \tag{27}$$

There is still some freedom in the choice of $\tilde{A}$, $\tilde{b}$, $\tilde{S}_f$, Δz and Δb. In the following section, a validation of this numerical technique using experimental data is presented. The criterion for the selection of the particular average values used is justified in the study of the steady solution next.

4.1.1. Numerical versus experimental results

Some results are presented for water flow in a prismatic rectangular channel containing bed variations. The test case was developed as a laboratory experiment by J.M. Hiver from the Free University of Brussels, Belgium. It consists of a constant width channel with an obstacle in the shape of a triangle. Initially, a gate placed at 15.5 m from the left end keeps water at rest upstream at a level of 0.75 m. Downstream of the gate, the channel is dry except for a pool of still water bounded by the obstacle and a downstream weir 0.15 m high. The gate is suddenly removed and the volume of water is released. The water wave advances over the flat bed first and over the adverse slope afterwards. Figs. 2 and 3 display some results at two times after the gate removal using the upwind and pointwise approaches for the discretization of the source terms. They show water profiles along the channel at times $t = 3$ and 10 s. They are not compared to any exact solution since the ideal dam-break flow exact solution is not applicable here where friction and slope changes are present and determinant. The friction term was

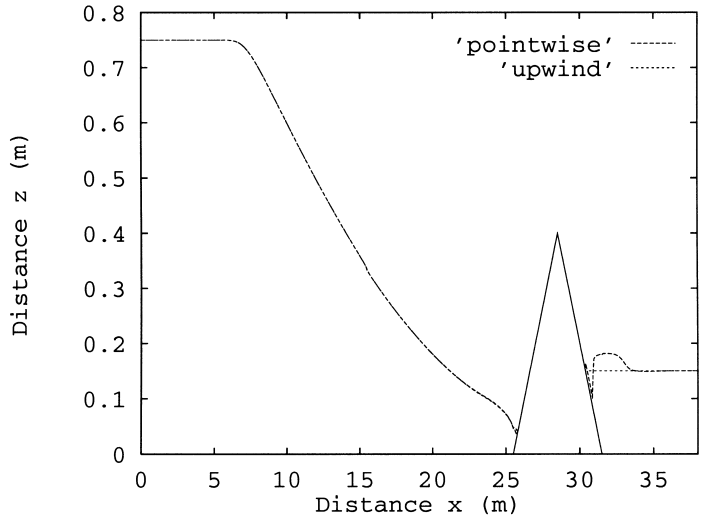

Fig. 2. Dam-break wave evolution. Water level. $N = 100$, $t = 3$ s.

included with a Manning roughness coefficient $n = 0.0125$ following the experimental team suggestion. Figs. 4 and 5 display a comparison of the results obtained with the upwind version against measured data at gauge points located 4 and 20 m from the gate, respectively.

4.1.2. Study of the steady solution: water at rest

In order to understand the different behaviour in these two figures, an analysis of the resulting schemes with upwind and pointwise discretizations of the source terms is done. This

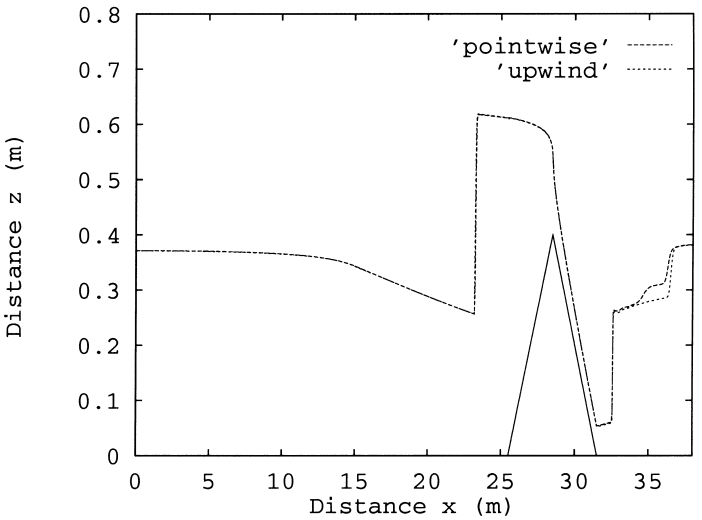

Fig. 3. Dam-break wave evolution.Water level. $N = 100$, $t = 10$ s.

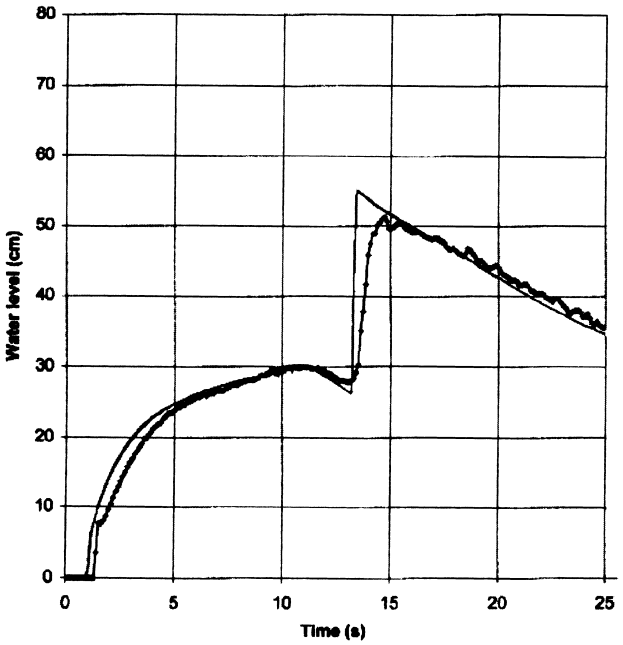

Fig. 4. Water level. Numerical results (thin line) versus experimental data (thick line) $x = 19.5$ m.

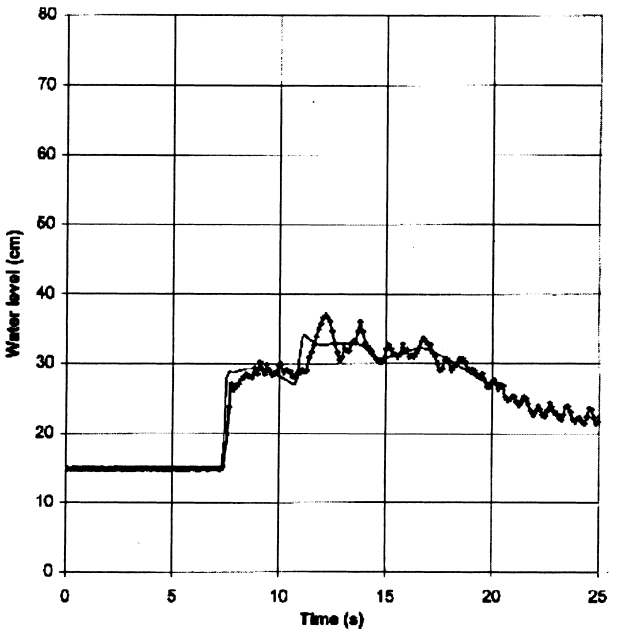

Fig. 5. Water level. Numerical results (thin line) versus experimental data (thick line) $x = 35.5$ m.

analysis is related with the C Property in [3], and with the definition of the "well-balanced scheme" in [8].

The numerical scheme can be represented by

$$\mathbf{U}_i^{n+1} = \mathbf{U}_i^n - \mathrm{LHS} + \mathrm{RHS}$$

where LHS and RHS denote for the node i the flux and source discretization, respectively. Then, for a stationary solution the scheme must verify

$$\mathrm{LHS} = \mathrm{RHS}.$$

For this test problem the flux discretization is

$$\mathrm{LHS} = \frac{\Delta t}{2\Delta x}\begin{pmatrix} -(\tilde{c}\Delta A)_{i+\frac{1}{2}} + (\tilde{c}\Delta A)_{i-\frac{1}{2}} \\ \left(\tilde{c}^2\Delta A\right)_{i+\frac{1}{2}} + \left(\tilde{c}^2\Delta A\right)_{i-\frac{1}{2}} \end{pmatrix}$$

The pointwise discretization of the source term is

$$\mathrm{RHS_p} = \frac{\Delta t}{\Delta x}\begin{pmatrix} 0 \\ -g\Delta x\left((Az_x)_i + \left(AS_f\right)_i\right) \end{pmatrix}$$

and the upwind discretization of the source term is

$$\mathrm{RHS_u} = \frac{\Delta t}{\Delta x}\begin{pmatrix} -\tilde{\beta}_{i+\frac{1}{2}} + \tilde{\beta}_{i-\frac{1}{2}} \\ \left(\tilde{c}\tilde{\beta}\right)_{i+\frac{1}{2}} + \left(\tilde{c}\tilde{\beta}\right)_{i-\frac{1}{2}} \end{pmatrix}.$$

where β is given by (27). It is easy to conclude that

$$\mathrm{LHS} - \mathrm{RHS_p} = \frac{\Delta t}{2\Delta x}\begin{pmatrix} -(\tilde{c}\Delta A)_{i+\frac{1}{2}} + (\tilde{c}\Delta A)_{i-\frac{1}{2}} \\ 0(\Delta x)^2 \end{pmatrix}$$

where the first component of $\mathrm{LHS} - \mathrm{RHS_p}$ is $0(\Delta x)$ and is a discretization of

$$-\Delta x\frac{\partial}{\partial x}\left(c\frac{\partial A}{\partial x}\right).$$

This term is responsible for the spurious wave in Figs. 2 and 3. Then, to vanish this term it should be necessary to reduce considerably Δx.

On the contrary, with the upwind approach we obtain $\mathrm{LHS} = \mathrm{RHS_u}$ for the choices

$$\Delta z = z_{i+1} - z_i \quad \tilde{h} = \frac{1}{2}(h_{i+1} + h_i) \quad \tilde{A} = \tilde{h}\tilde{b}$$

It is worth noting here that the C Property supplies the constraint on the average values

related to the source terms in the same way as the U Property in Roe's method allows the definition of the standard Roe average.

4.2. Non-prismatic channel: $\mathbf{F} = \mathbf{F}(\mathbf{x}, \mathbf{U})$

As commented before, in this case the source term can be redefined

$$\hat{\mathbf{R}} = \mathbf{R} - \mathbf{V} = \left(0, \frac{gA^2}{b^2} b_x + gAS_0\right)^{\mathrm{T}} \tag{28}$$

If the system is modified in this sense, so that it retains in the left-hand side, only the terms fulfilling condition (1), then a different source term is projected, giving in general

$$\hat{\mathbf{R}} = \begin{pmatrix} 0 \\ g\left(-\tilde{A}z_x - \tilde{A}\tilde{S}_f + \frac{\tilde{A}^2}{\tilde{b}^2} b_x\right) \end{pmatrix} = \frac{1}{\Delta x}\left(\tilde{\beta}_1 \begin{pmatrix} 1 \\ \tilde{u} + \tilde{c} \end{pmatrix} + \tilde{\beta}_2 \begin{pmatrix} 1 \\ \tilde{u} - \tilde{c} \end{pmatrix}\right)$$

that is

$$\tilde{\beta}_1 = -\tilde{\beta}_2 = \tilde{\beta}$$

$$\tilde{\beta} = \frac{\Delta x}{2\tilde{c}} g\left(-\tilde{A}z_x\tilde{A}\tilde{S}_f + \frac{\tilde{A}^2}{\tilde{b}^2} b_x\right) = \frac{g}{2\tilde{c}}\left(-\tilde{A}\Delta z - \tilde{A}\Delta x\tilde{S}_f + \frac{\tilde{A}^2}{\tilde{b}^2}\Delta b\right). \tag{29}$$

Note that the only difference is a factor 2 in the last term. In the next section, the numerical results for an academic still water test case are presented. The determination of the average values is justified later.

4.2.1. Numerical results

The test case consists of a channel of rectangular cross-section with variable width and bottom level. The variations of width with distance are displayed in Fig. 6. A constant 12 m level of water at rest is imposed at $t = 0$. The analytical solution is zero discharge and a constant water surface level everywhere, as in the previous case.

In the pointwise version of the scheme's implementation, the following was used

$$S_{0i} \approx \frac{1}{2}\left(S_{0i+\frac{1}{2}} + S_{0i-\frac{1}{2}}\right) \qquad S_{0i+\frac{1}{2}} = -\frac{z_{i+1} - z_i}{\Delta x}$$

$$I_{2i} \approx \frac{1}{2}\left(I_{2i+\frac{1}{2}} + I_{2i-\frac{1}{2}}\right), \qquad I_{2i+\frac{1}{2}} = \frac{1}{2} h_i^2 \frac{b_{i+1} - b_i}{\Delta x}.$$

Fig. 7 corresponds to the results supplied by this pointwise version. Fig. 8 has been obtained using Roe's scheme and upwind source term discretization but without corrected flux, that is, based on definitions (11) and (27). As the picture makes plain, the algorithm fails to reproduce

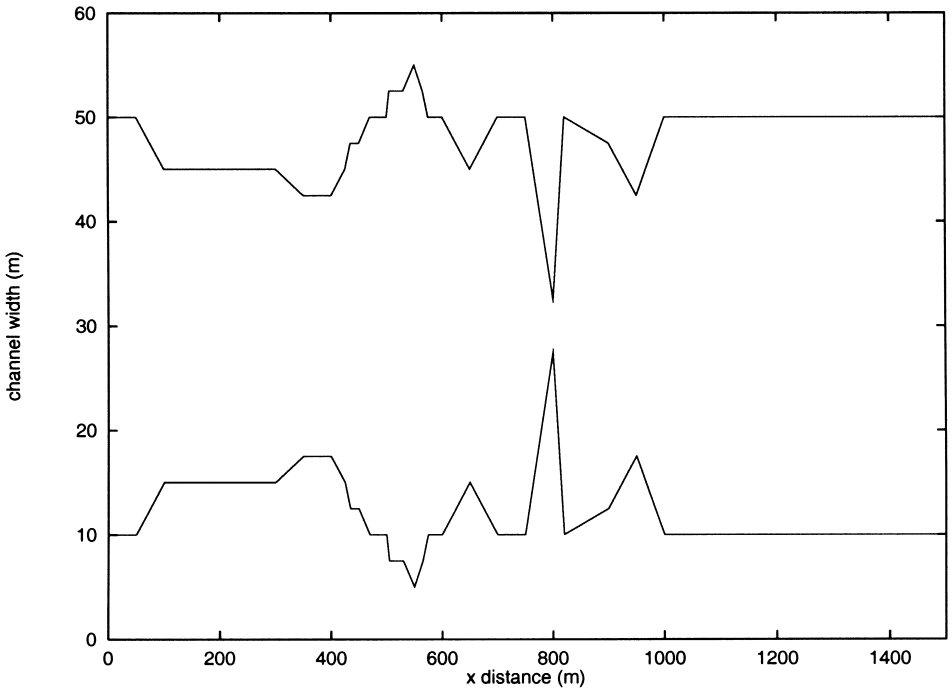

Fig. 6. Channel width variation.

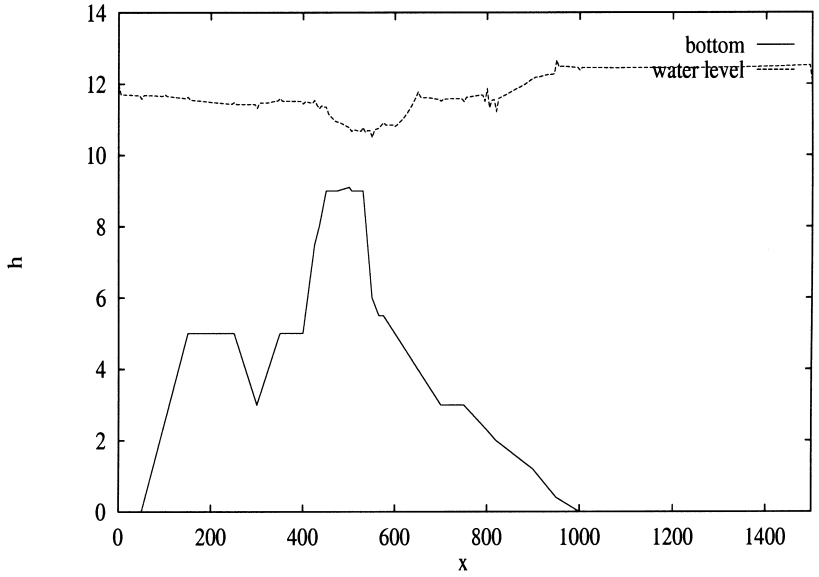

Fig. 7. Steady state in the channel with variable width. Pointwise source terms with non-corrected flux. $N = 300$, $t = 200$ s.

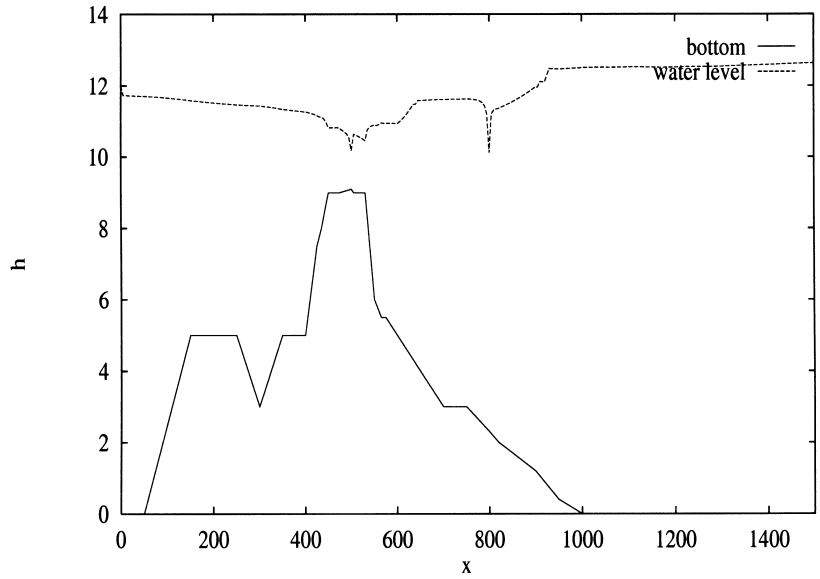

Fig. 8. Steady state in the channel with variable width. Upwind source terms with non-corrected flux. $N = 300$, $t = 200$ s.

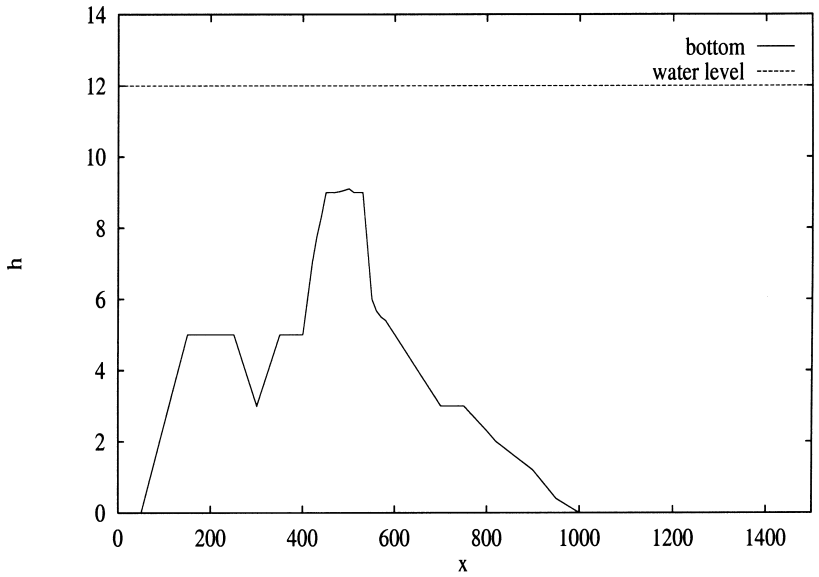

Fig. 9. Steady state in the channel with variable width. Upwind source terms with non-corrected flux. $N = 300$, $t = 200$ s.

the exact steady state. The application of the corrections proposed in this report, (11) and (28) leads to the exact result. It is plotted in Fig. 9.

4.2.2. Study of the steady case: water at rest

The importance of this factor, is again related to what happens at the discrete level when equilibrium is sought (see [6]). A zero velocity steady state will be assumed in a rectangular channel with variations in bed level and width, i.e., $v = Q = 0$, $h \neq cte$, $z \neq cte$, $h + z = cte$, $b \neq cte$. Using Eqs. (6) and (7) and the fact that in this case

$$\tilde{\alpha}_1 = \tilde{\alpha}_2 = \frac{\Delta A}{2}.$$

the flux discretization (LHS) gives for node i

$$\mathrm{LHS} = \frac{\Delta t}{2\Delta x}\begin{pmatrix} -(\tilde{c}\Delta A)_{i+\frac{1}{2}} + (\tilde{c}\Delta A)_{i-\frac{1}{2}} \\ \left(\tilde{c}^2\Delta A\right)_{i+\frac{1}{2}} + \left(\tilde{c}^2\Delta A\right)_{i-\frac{1}{2}} \end{pmatrix}$$

On the other hand, the discrete source terms (RHS), from Eq. (11) or (12), supply a contribution

$$\mathrm{RHS} = \frac{\Delta t}{\Delta x}\begin{pmatrix} -\tilde{\beta}_{i+\frac{1}{2}} + \tilde{\beta}_{i-\frac{1}{2}} \\ \left(\tilde{c}\tilde{\beta}\right)_{i+\frac{1}{2}} + \left(\tilde{c}\tilde{\beta}\right)_{i-\frac{1}{2}} \end{pmatrix}.$$

Using Eq. (26) for $\tilde{c}$ and the average values

$$\Delta z = z_{i+1} - z_i \qquad \Delta b = b_{i+1} - b_i$$

$$\tilde{h} = \frac{1}{2}(h_{i+1} + h_i) \qquad \tilde{b} = \frac{1}{2}(b_{i+1} + b_i)$$

$$\tilde{A} = \tilde{h}\tilde{b} \tag{30}$$

it is easy to verify that LHS = RHS only if $\tilde{\beta}$ is given by Eq. (28). It could also be verified that, in case of constant width channel, the discrete equilibrium is also achieved.

Having found a solution to achieve equilibrium when using Roe's fluctuation signal scheme in the presence of geometrical source terms, we would like to know whether it would hold when using the (non corrected) numerical flux approach instead. For this purpose, the updating of nodal point i is written as

$$\mathbf{U}_i^{n+1} = \mathbf{U}_i^n - \underbrace{\frac{\Delta t}{\Delta x}\left(f^*_{i+\frac{1}{2}} - f^*_{i-\frac{1}{2}}\right)}_{\mathrm{LHS}} + \underbrace{\Delta t\left(\frac{1}{2}\left(\boldsymbol{\psi}_{\mathrm{L}}\right)_{i-\frac{1}{2}} + \frac{1}{2}\left(\boldsymbol{\psi}_{\mathrm{R}}\right)_{i+\frac{1}{2}}\right)}_{\mathrm{RHS}}. \tag{31}$$

The answer is that the equilibrium is broken with the definition of β given either by Eq. (27) or (29). Figs. 10 and 11 display the results with (29).

In order to understand what happens, an analysis of the discretization (31) trying to enforce equilibrium ($\mathbf{U}_i^{n+1} = \mathbf{U}_i^n$) will be repeated here. With the definition of the quantities LHS and RHS, we require, as before,

$$\text{LHS} = \text{RHS}$$

for equilibrium.

Using again the zero velocity steady state, the numerical flux balance gives

$$\text{LHS} = \frac{\Delta t}{2\Delta x}\begin{pmatrix} -(\tilde{c}\Delta A)_{i+\frac{1}{2}} + (\tilde{c}\Delta A)_{i-\frac{1}{2}} \\ \left(\frac{gA^2}{2b}\right)_{i+1} - \left(\frac{gA^2}{2b}\right)_{i-1} \end{pmatrix}.$$

On the other hand, the discrete source terms (RHS)

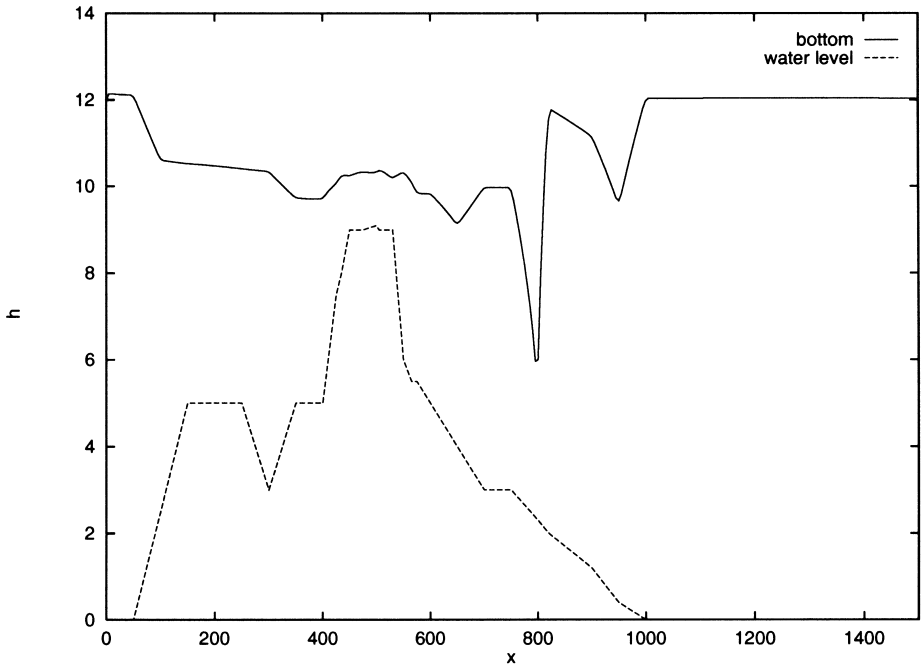

Fig. 10. Water level at steady state in the channel with variable width. Upwind source terms with non-corrected numerical flux. $N = 300$, $t = 200$ s.

$$\mathrm{RHS} = \frac{\Delta t}{\Delta x}\begin{pmatrix} -\tilde{\beta}_{i+\frac{1}{2}} + \tilde{\beta}_{i-\frac{1}{2}} \\ \left(\tilde{c}\tilde{\beta}\right)_{i+\frac{1}{2}} + \left(\tilde{c}\tilde{\beta}\right)_{i-\frac{1}{2}} \end{pmatrix}.$$

It could be said, strictly speaking, the numerical flux function has to be changed in this case. It can nevertheless still be expressed in terms of the numerical flux (9) if only the corrections to the numerical flux are also passed to the right hand side.

It is simple to try and verify that the previous choice (30) for the average values together with the definition of β (29) produces the balance in the first components (mass equation) but not in the second components (momentum equation).

Equilibrium in the second components can be achieved with the original definition of β, (27) and the averages

$$\tilde{h} = \sqrt{h_{i+1}h_i} \qquad \tilde{A} = \frac{1}{2}(b_{i+1}h_{i+1} + b_i h_i). \tag{32}$$

This choice however perturbs the mass balance. Full equilibrium in this case requires double definition of the coefficient and averages that would not be easy to obtain in unsteady cases. By using Eqs. (29) and (30) for the mass equation and Eqs. (27) and (31) for the momentum

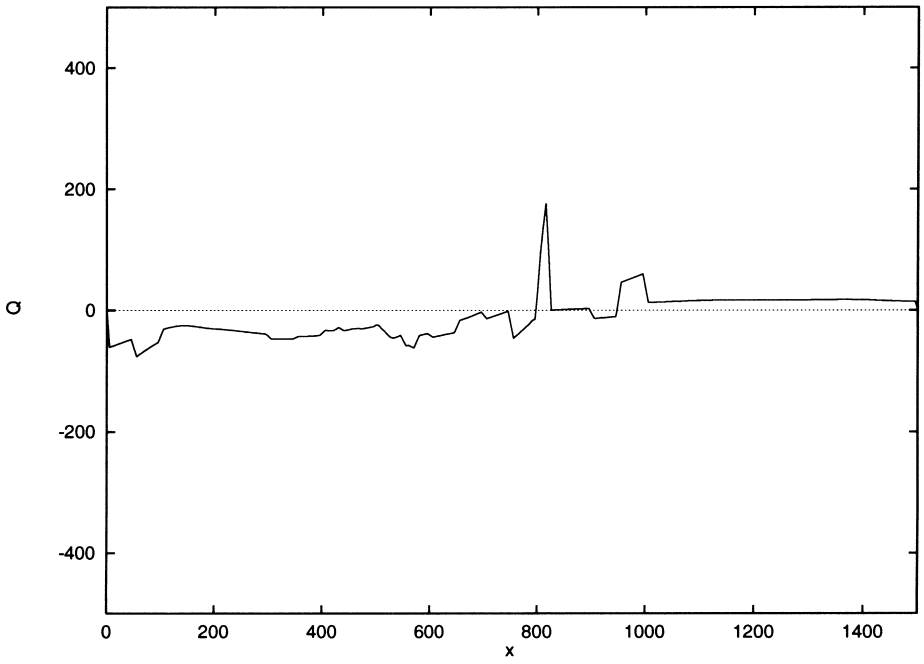

Fig. 11. Discharge at steady state in the channel with variable width. Upwind source terms with non-corrected numerical flux. $N = 300$, $t = 200$ s.

equation, the steady state is satisfactorily achieved as Figs. 12 and 13 show. The use of the new corrections associated with the numerical flux achieve the desired exact solution.

5. Application to a 1D solute transport test case

A different test case has been selected to illustrate the details of the techniques referred in this paper for a scalar case. The test case that has been used for this purpose is a Riemann problem in the context of 1D shallow water flow. It is characterized by discontinuous initial water levels at rest and discontinuous initial distribution of a solute concentration in the water.

This problem is generated by the 1D shallow water equations previously presented and a solute mass conservation equation:

$$\frac{\partial h}{\partial t} + \frac{\partial q}{\partial x} = 0$$

$$\frac{\partial q}{\partial t} + \frac{\partial}{\partial x}\left(u^2 h + g\frac{h^2}{2}\right) = 0$$

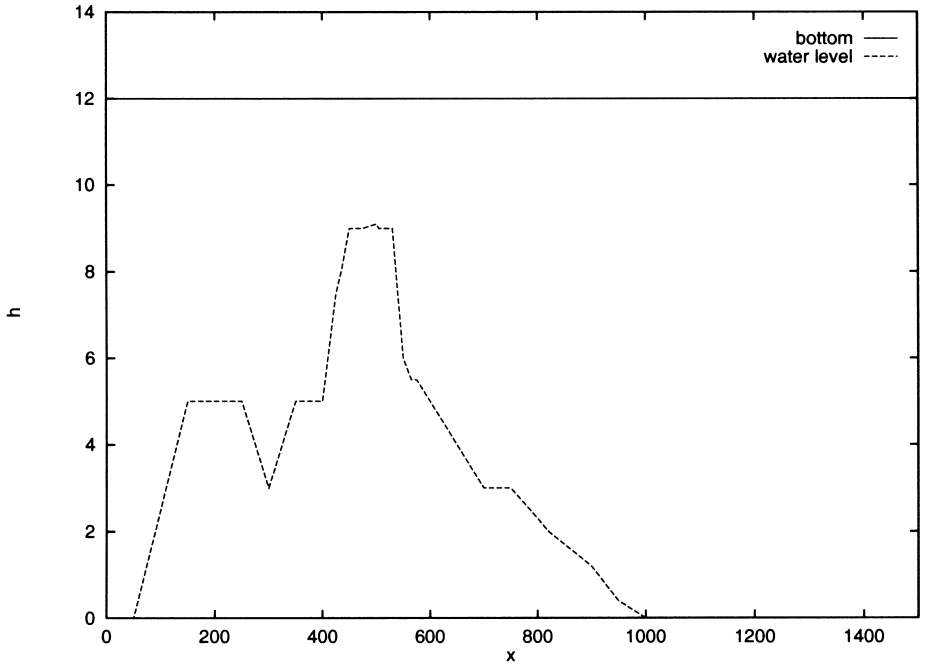

Fig. 12. Water level at steady state in the channel with variable width. Upwind source terms with corrected numerical flux. $N = 300$, $t = 200$ s.

$$\frac{\partial c}{\partial t} + u\frac{\partial c}{\partial x} = 0 \tag{33}$$

where h is the water depth, u is the depth averaged water velocity and $q = uh$ represents the unit discharge, c represents the depth averaged solute concentration and g is the acceleration due to gravity. Note that the abuse in notation given by the repetition of the name c for a new variable is due to the fact that the wave surface celerity will not be used any more in what follows. The initial conditions are

$$h(x,0) = \begin{cases} h_L & \text{if } x \leq \dfrac{L}{2} \\ h_R & \text{if } x > \dfrac{L}{2} \end{cases}$$

$$q(x,0) = 0.$$

$$c(x,0) = \begin{cases} c_L & \text{if } x \leq \dfrac{L}{2} \\ c_R & \text{if } x > \dfrac{L}{2} \end{cases} \tag{34}$$

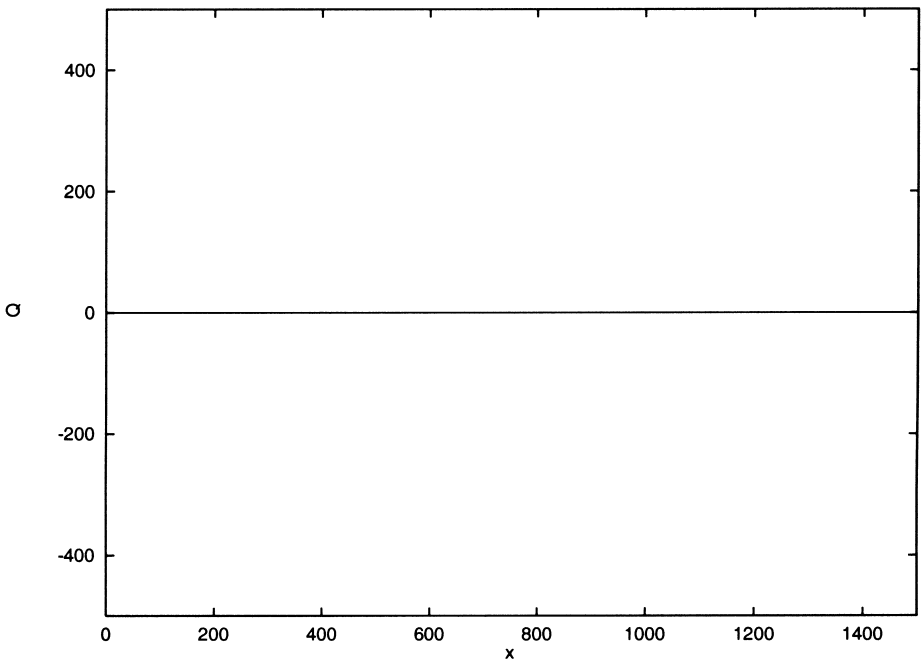

Fig. 13. Discharge at steady state in the channel with variable width. Upwind source terms with corrected numerical flux. $N = 300$, $t = 200$ s.

Calculation times were used so as to avoid interaction with the extremities of the channel. The boundary conditions are then trivial.

This idealized dam-break problem was chosen because it is a classical example of nonlinear flow with shocks to test conservation in numerical schemes and, at the same time, has an exact solution. The coupling of the equations in the system (33) is such that the dynamics of the concentration depends on the water flow dynamics but the hydraulic problem is independent of the concentration. The exact dam-break flow solution consists of a sharp shock wave advancing downstream and a smooth depression wave propagating upstream. It can be shown [4] that the exact solution for the wave generated by the initial discontinuity in concentration is a step like wave that progresses at a slower rate than the water wave. The performance of the first order upwind scheme with Roe's discretization for the solution of the dam-break water flow has previously been tested.

The contribution of this section is to analyze the discretization of the partial differential equation for the concentration in (32). In order to do that, we start recalling the general procedure for the numerical resolution of a scalar conservation law

$$\frac{\partial c}{\partial t} + \frac{\partial f(c)}{\partial x} = 0, \qquad \lambda = \frac{\partial f(c)}{\partial c} \tag{35}$$

in a regular discrete mesh $\{x_i,\ i = 1, N\}$ by means of the first order upwind scheme. The average discrete advection velocity at an interface $x_{i+\frac{1}{2}}$ has to be defined

$$\tilde{\lambda}_{i+\frac{1}{2}} = \begin{cases} \dfrac{f_{i+1} - f_i}{c_{i+1} - c_i} & \text{if } c_{i+1} - c_i \neq 0 \\ \lambda_i & \text{if } c_{i+1} - c_i = 0 \end{cases} \tag{36}$$

so that contributions of different sign emerge from the interface according to the sign of $c_{i+\frac{1}{2}}$

$$\Delta f^{\pm}_{i+\frac{1}{2}} = \lambda^{\pm}_{i+\frac{1}{2}} \Delta c_{i+\frac{1}{2}}$$

and the function at node i for instance, is updated in time Δt, according to contributions from left and right.

$$c_i^{n+1} = c_i^n - \frac{\Delta t}{\Delta x}\left(\Delta f^{+}_{i-\frac{1}{2}} + \Delta f^{-}_{i+\frac{1}{2}}\right). \tag{37}$$

Usually, a numerical flux is defined and the above re-expressed

$$c_i^{n+1} = c_i^n - \frac{\Delta t}{\Delta x}\left(f^{*}_{i+\frac{1}{2}} - f^{*}_{i-\frac{1}{2}}\right) \tag{38}$$

with

$$f^{*}_{i+\frac{1}{2}} = \frac{1}{2}(f_{i+1} + f_i) - \frac{1}{2}|\lambda_{i+\frac{1}{2}}|\Delta c_{i+\frac{1}{2}}.$$

These are the two versions of the scheme corresponding to the signal and flux methods seen in Section 2.

In what follows, we try to apply these ideas to the partial differential equation for the concentration:

$$\frac{\partial c}{\partial t} + u\frac{\partial c}{\partial x} = 0 \tag{39}$$

The test case selected corresponds to initial values for the water depth ratio h_L:h_R of 10:1 and for the concentration ratio c_L:c_R of 0.4:0. The results obtained with different options are considered separately and numbered for the sake of clarity in the dicussion.

Figs. 14–16 show results for the concentration wave obtained with the signal scheme. Since the equation we are dealing with is not in the form of a conservation law, we do not have a physical flux whose discrete values f_i can be used to define the average advection velocity as in Eq. (36). So, the first question is about the most convenient way to define the average advection velocity $\tilde{\lambda}_{i+\frac{1}{2}}$.

1. Fig. 14 was obtained using

$$\tilde{\lambda}_{i+\frac{1}{2}} = \frac{1}{2}(u_i + u_{i+1}),$$

where u_i is the discrete velocity of the shallow water equations and then

$$\tilde{\lambda}^{\pm}_{i+\frac{1}{2}} = \frac{1}{2}\left(\tilde{\lambda}_{i+\frac{1}{2}} \pm |\tilde{\lambda}_{i+\frac{1}{2}}|\right)$$

The numerical results from this option will be used as reference results to compare with those obtained from the other options.

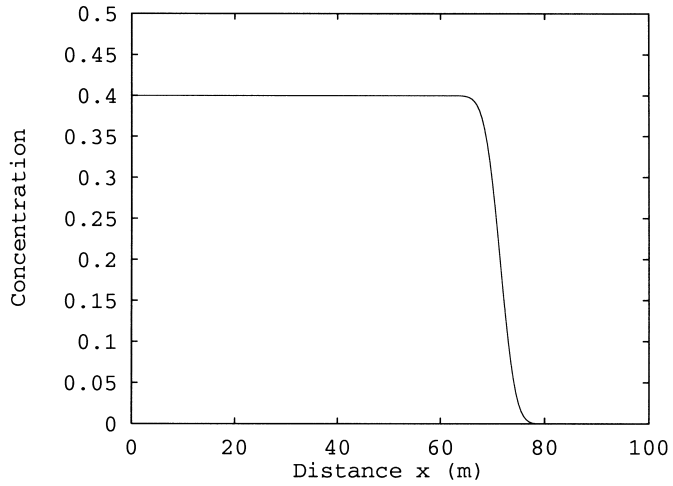

Fig. 14. Options 1 and 3. Roe's signal scheme: $\tilde{\lambda}_{i+\frac{1}{2}} = \frac{1}{2}(u_i + u_{i+1})$.

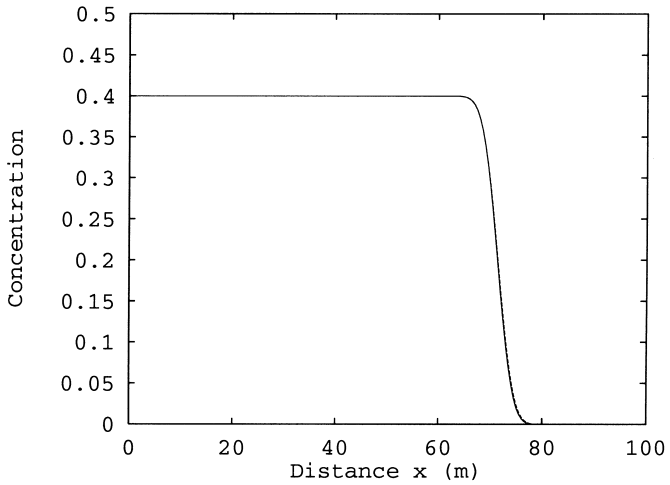

Fig. 15. Option 2. Roe's signal scheme: $\tilde{\lambda}_{i+\frac{1}{2}} = \tilde{u}_{i+\frac{1}{2}}$ (continuous line).

2. The numerical results are analogous if the average velocity is taken as that supplied by the water flow Riemann solver, that is,

$$\tilde{\lambda}_{i+\frac{1}{2}} = \tilde{u}_{i+\frac{1}{2}}$$

and $\tilde{u}$ is defined in (25). This is shown in Fig. 15 with continuous line and is practically coincident with the discontinuous line from option 1.

The formulation for the concentration equation as a conservation law is

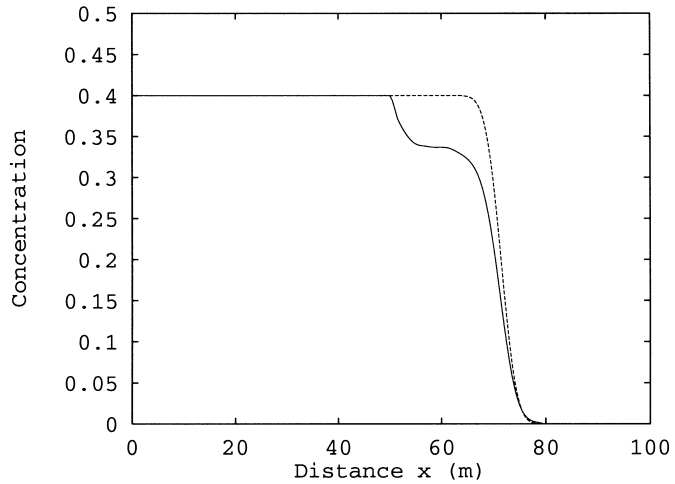

Fig. 16. Option 4. Roe's signal scheme. Incorrect flux formulation (continuous line).

$$\frac{\partial c}{\partial t} + \frac{\partial cu}{\partial x} = c\frac{\partial u}{\partial x} \tag{40}$$

where the introduced flux $f(x, c) = u(x, t)c(x, t)$ implies the existence of a source term. And due to the fact that $f = f(x, c)$ and not only $f = f(c)$, we have one V term like in Eq. (14), more precisely $V = c\frac{\partial u}{\partial x}$.

3. Roe's signal scheme with this conservative formulation induces the option to apply the development expressed in Section 2.3, to upwind and modify the physical flux, which is equivalent to the definition of $\tilde{\lambda}_{i+\frac{1}{2}}$ proposed in option 1, and then upwind the final source term. Nevertheless, this option is actually the same as the first one, because the correction of the flux, V, cancels the source term and returns to the non-conservative formulation of the equation.
4. It is obvious that the bad assumption for the Roe's signal scheme is to consider $f_i(x, c) = (uc)_i$, and to replace this function in (36), without modifying the flux. Fig. 16 shows the bad results versus those from option 1.

   Figs. 17 and 18 represent the solution obtained with Roe's numerical flux scheme. We only need to consider the flux because, as it has been mentioned, the final source term is null.
5. Fig. 17 corresponds to the modified numerical flux given by Eqs. (17) and (18) which involve the correction term

$$V_{i+\frac{1}{2}} = c_{i+\frac{1}{2}}\Delta u_{i+\frac{1}{2}}$$

   and it shows the correct results. The numerical results are identical to those from option 1.
6. Fig. 18 corresponds to a case in which (36) has been applied based on a physical flux defined as $f(x, c) = (uc)$, that is without flux modification. As it has been established in Section 2.3, this provides incorrect results. In this figure, the comparison with the results in Fig. 14 is done again.

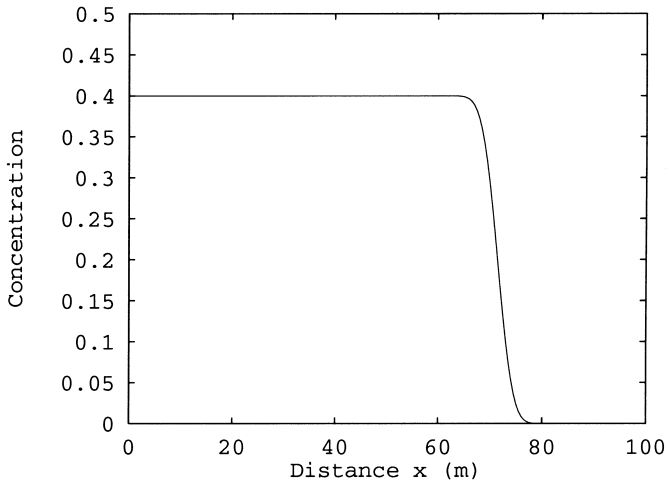

Fig. 17. Option 5. Roe's numerical flux scheme. Modified flux (continuous line).

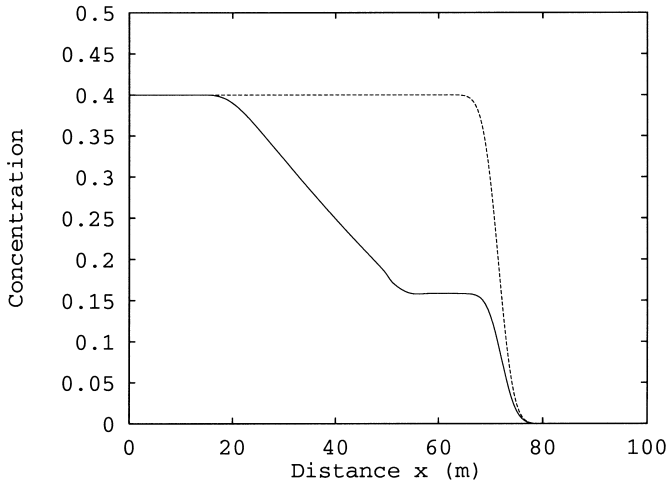

Fig. 18. Option 6. Roe's numerical flux scheme. Modified flux (continuous line).

6. Conclusions

The present work leads to the conclusion of the importance of the careful upwind treatment of the source terms when dealing with variable geometries in the context of Riemann solver based numerical schemes.

The extension of the formulation of Roe's discretization for homogeneous systems to systems involving source terms is not straightforward in general. Some differences arise between the differential and the discrete formulation of the equations. The flux difference splitting has to be performed retaining only the part depending on the conserved variables to represent the convective flux. All other dependences are to be moved to modify the source terms of the differential equations.

Two formulations of Roe's scheme have been presented, one based on a signal approach and the other involving the definition of a numerical flux function. Both approaches require a proper definition of the flux difference splitting. The scalar example on 1D advection of a concentration in water highlights the applicability of these concepts to conservation laws, in which, the flux function is not only a function of the conserved variables but also depends on the spatial variable.

The work presented deals only with rectangular geometries. Investigations in course indicate that the same kind of corrections must be applied to other geometries, leading to similar successful results. Future work will address this aspect as well as the correct numerical treatment of source terms when using a second-order scheme for the flux discretization.

Acknowledgements

The first author is very grateful to Prof. M.J. Baines and Dr. M.E. Hubbard for many interesting discussions.

References

[1] Abbott MB. Computational hydraulics. Worcester: Ashgate, 1992.
[2] Alcrudo F, Garcia-Navarro P. Flux-difference splitting for 1D open channel flow equations. Int J of Numerical Methods in Fluids 1992;14:1009–18.
[3] Bermudez A, Vazquez ME. Upwind methods for hyperbolic conservation laws with source terms. Computers and Fluids 1994;8:1049–71.
[4] Bradford SF, Katopodes ND, Parker G. Characteristic analysis of turbid underflows. Journal of Hydraulic Engineering 1997;123:420–31.
[5] Cunge JA, Holly FM, Verwey A. Practical aspects of computational river hydraulics. Massachusetts: Massachusetts Pitman, 1980.
[6] Garcia-Navarro P. Workshop on dam-break flow modelling: some results for 1D test cases. Internal Report, Fluid Mechanics, CPS, University of Zaragoza, 1996.
[7] Glaister P. Approximate Riemann solutions of the shallow water equations. Journal of Hydraulic Research 1988;26:293–306.
[8] Greenberg JM, Leroux AY. A well balanced scheme for the numerical processing of source terms in hyperbolic equations. SIAM Journal of Numerical Analysis 1996;33:1–16.
[9] Nujic M. Efficient implementation of non-oscillatory schemes for the computation of free-surface flows. Journal of Hydraulic Research 1995;33:101–11.
[10] Roe PL. Approximate Riemann solvers, parameter vectors and difference schemes. Journal of Computational Physics 1981;43:357–72.
[11] Vazquez Cendon ME. Estudio de esquemas descentrados para su aplicacion a las leyes de conservacion hiperbolicas con terminos fuente. Tesis Doctoral, Universidad de Santiago de Compostela, 1994.